Dual response fluorescent sensor for HNO and S^{2-} ions using Cu(II) complex based probe assistant with detailed DFT studies.

Ananya Dutta[a], Rabiul Alam[a], Abu Saleh Musha Islam[a], Arpan Dutta[a] and Mahammad Ali[a,b*]

[a]Department of Chemistry Jadavpur University, Kolkata 700 032, India; Fax: 91-33-2414-6223, E-mail: m_ali2062@yahoo.com, mali@chemistry.jdvu.ac.in

[b]Vice-Chancellor, Aliah University, II-A/27, Action Area II, Newtown, Action Area II, Kolkata, West Bengal 700160,

Supporting Information for Publication

17.	Selected parameters for the vertical excitation (UV-VIS absorptions) of **[$Cu^{II}(L^2)Cl$].**	**Table S3**
18.	Selected parameters for the vertical excitation (UV-VIS absorptions) of **[$Cu^{I}(L^2)$].**	**Table S4**

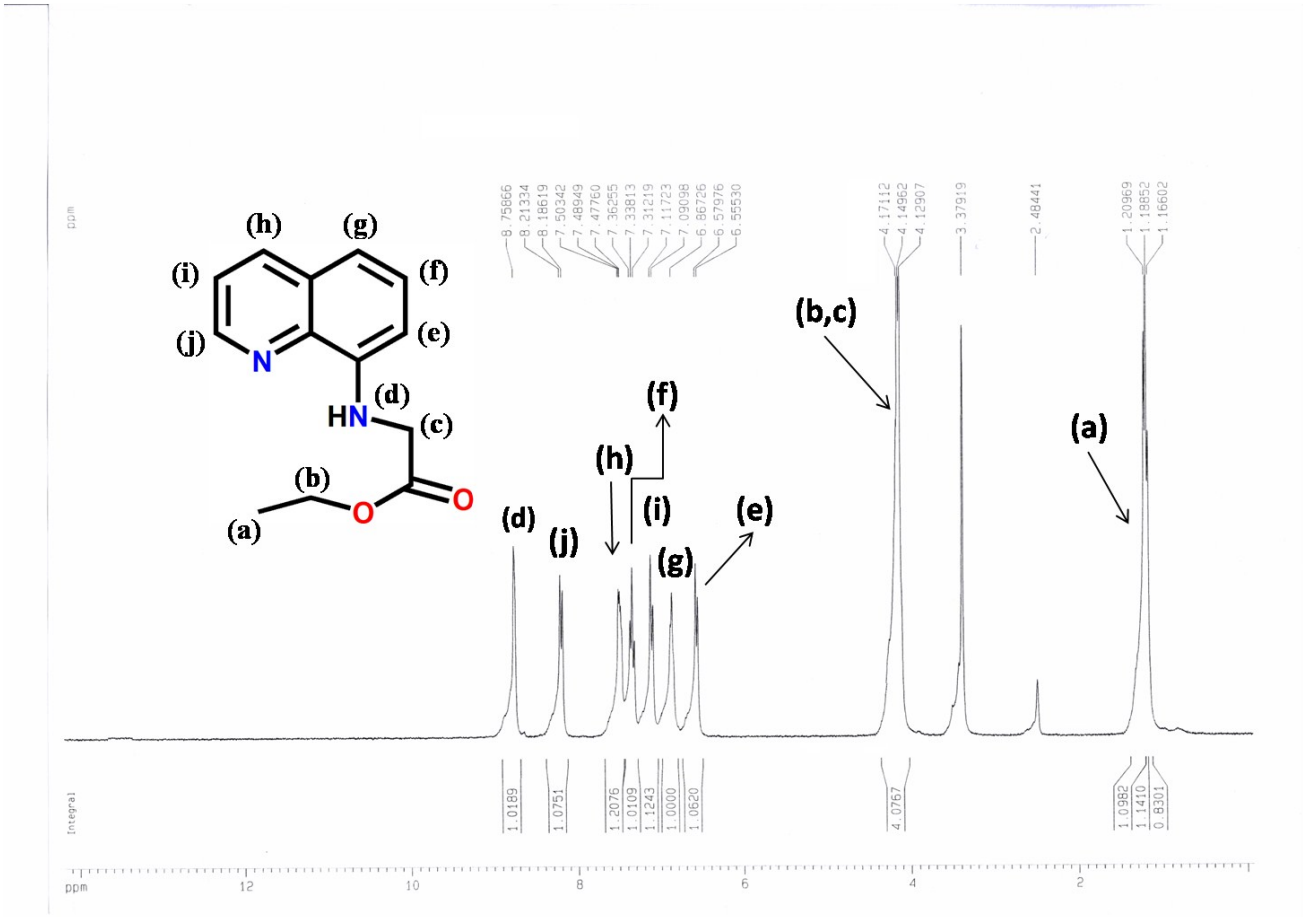

Fig.S1.^{1}H NMR spectrum of spectrum of(**L**[1]) in DMSO-d_6.

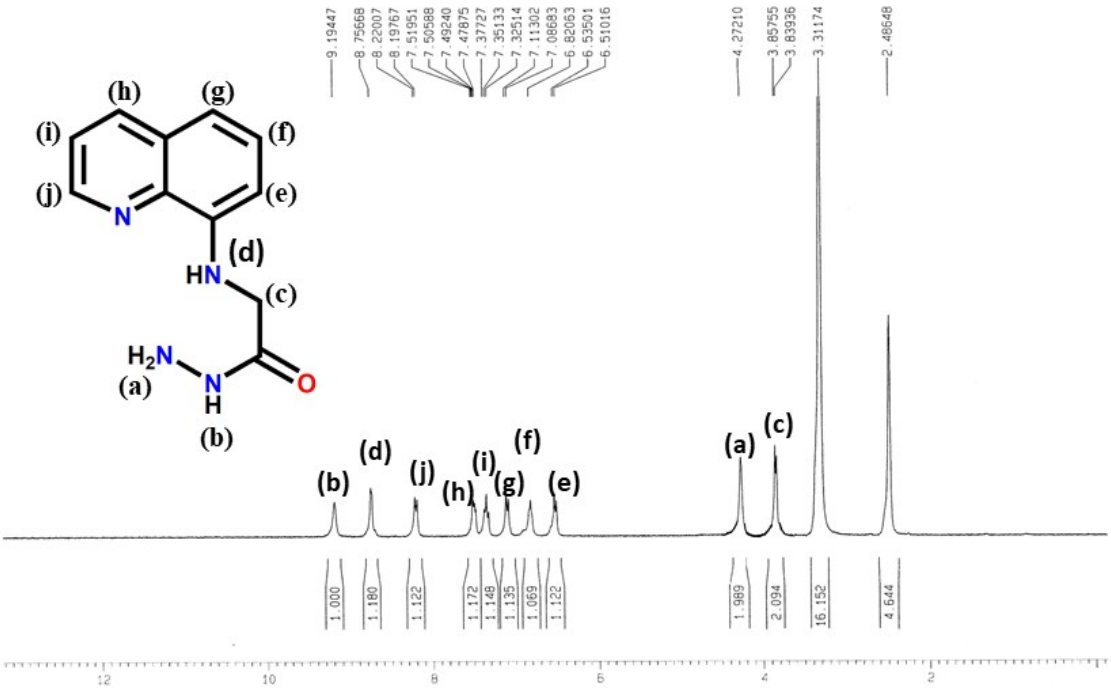

Fig. S1a.^{1}H NMR spectrum of spectrum of(**L^{2}**) in DMSO-$d_{6.}$

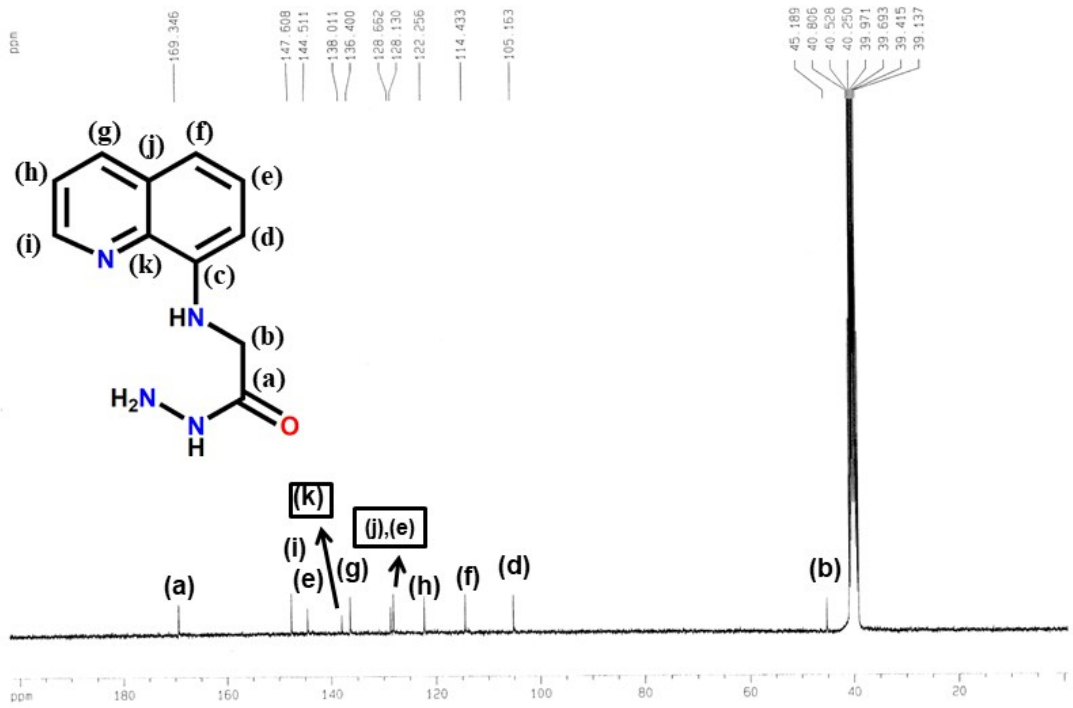

Fig.S2. ^{13}C NMR spectrum of **L^2** in DMSO-d_6 (300Mz).

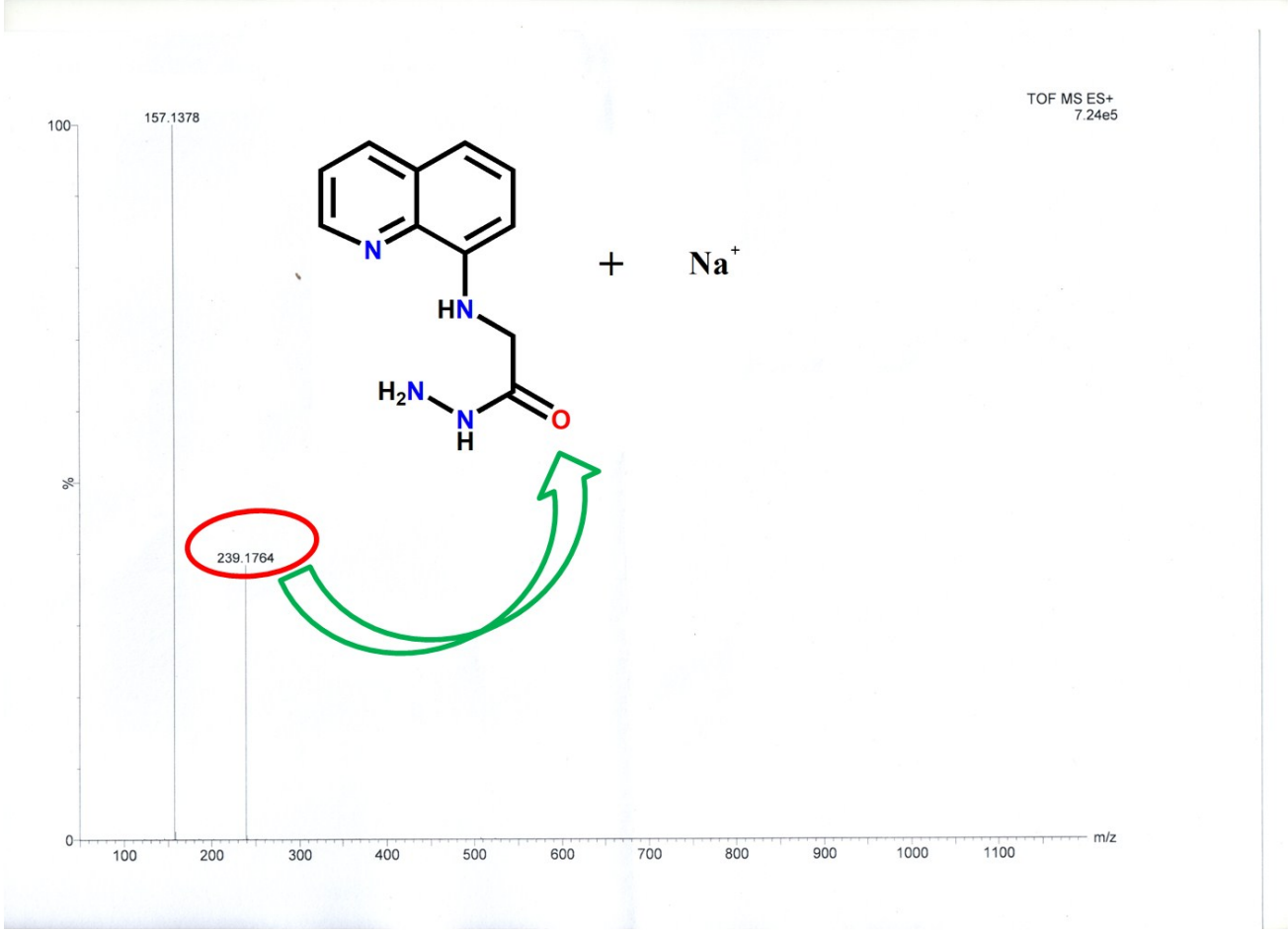

Fig. S3. Mass spectrum of **L²** in MeCN.

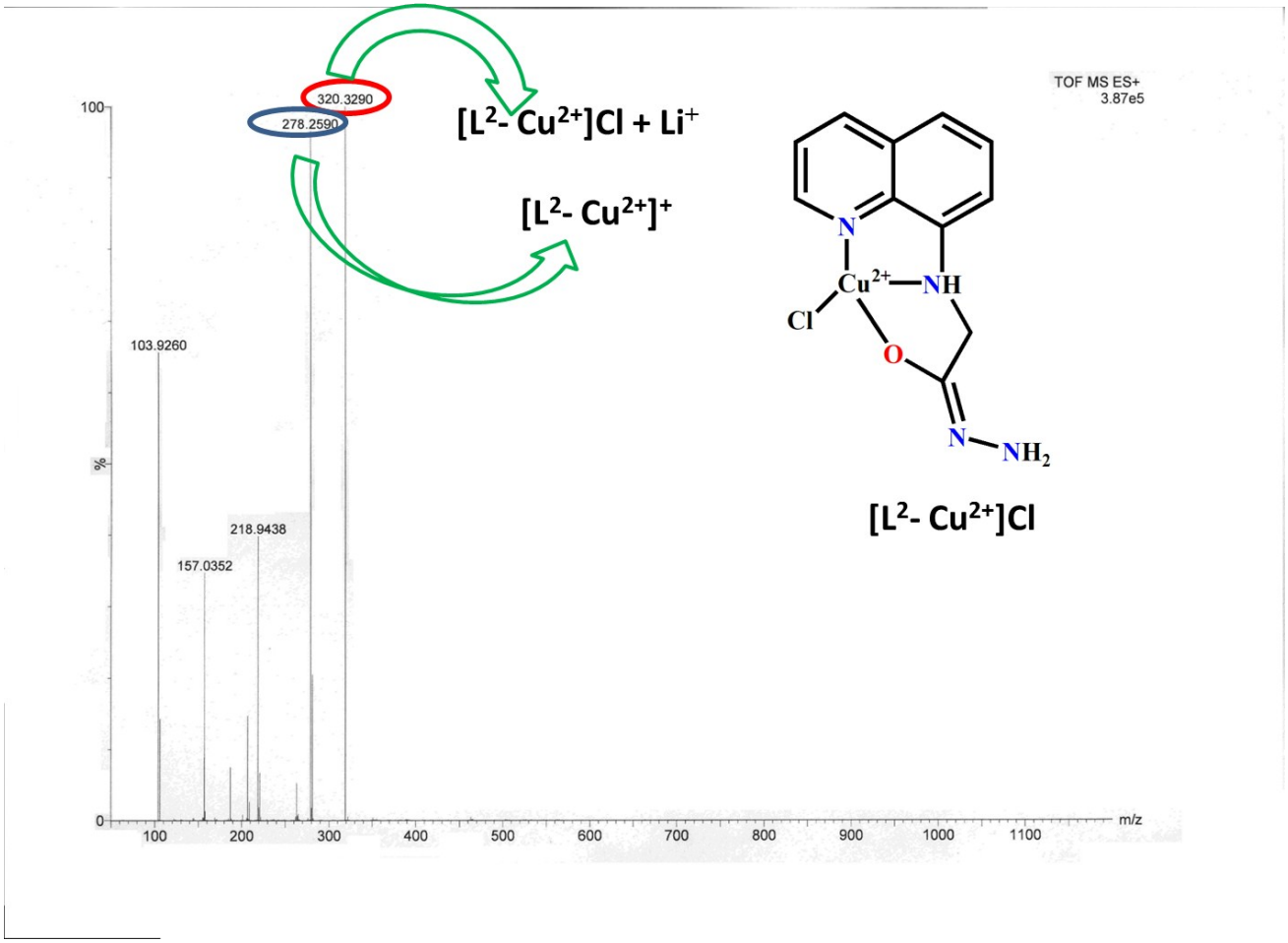

Fig. S3a. Mass spectrum of [**Cu(L^2)Cl**] in MeOH.

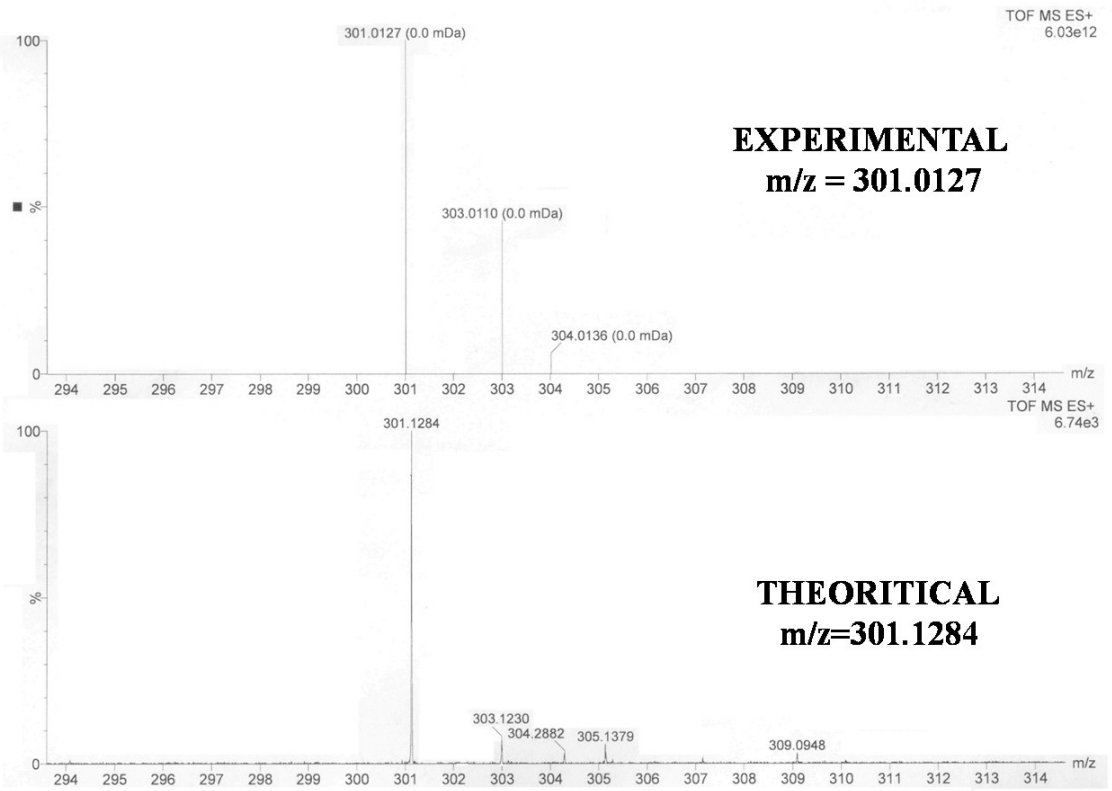

Fig. S3b. Mass spectrum of [**Cu(L^2)Cl]+ Na$_2$N$_2$O$_3$** in MeCN and H_2O.

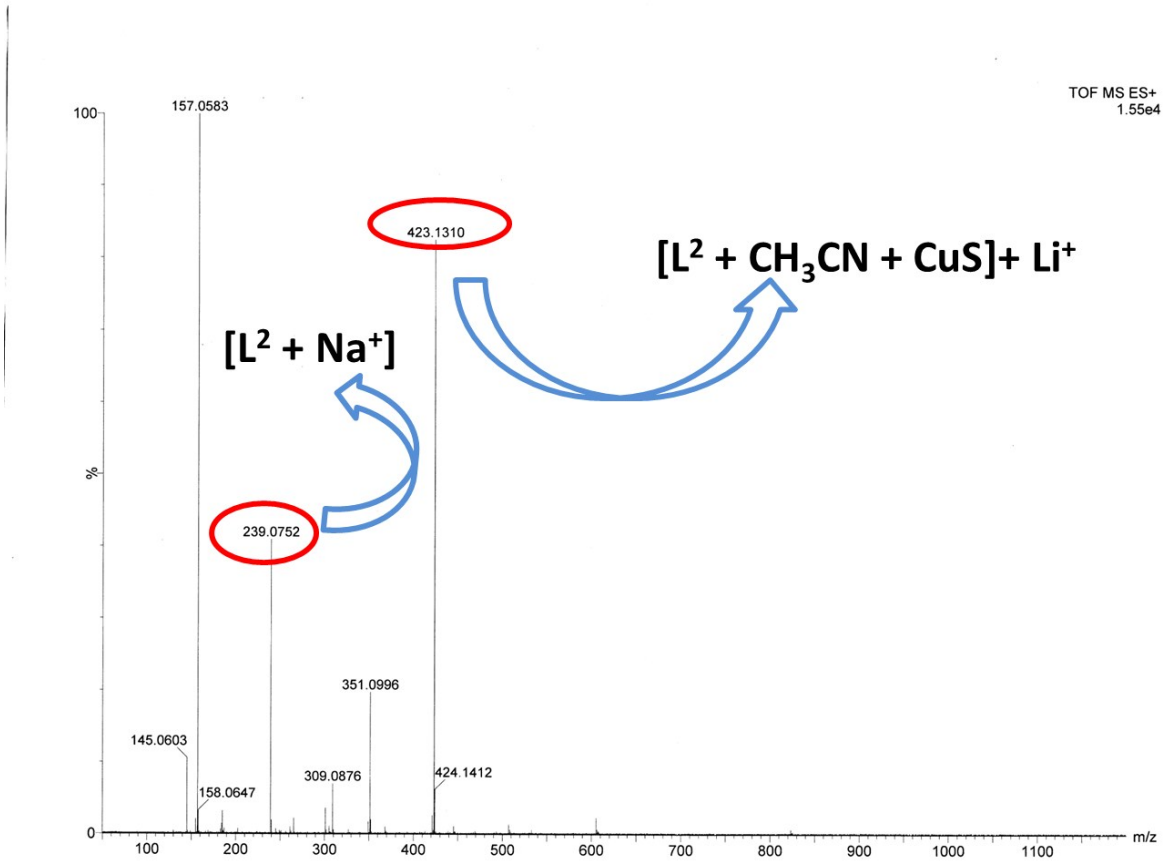

Fig. S3c. Mass spectrum of **Cu-L^2**+ Na_2S in MeCN and H_2O

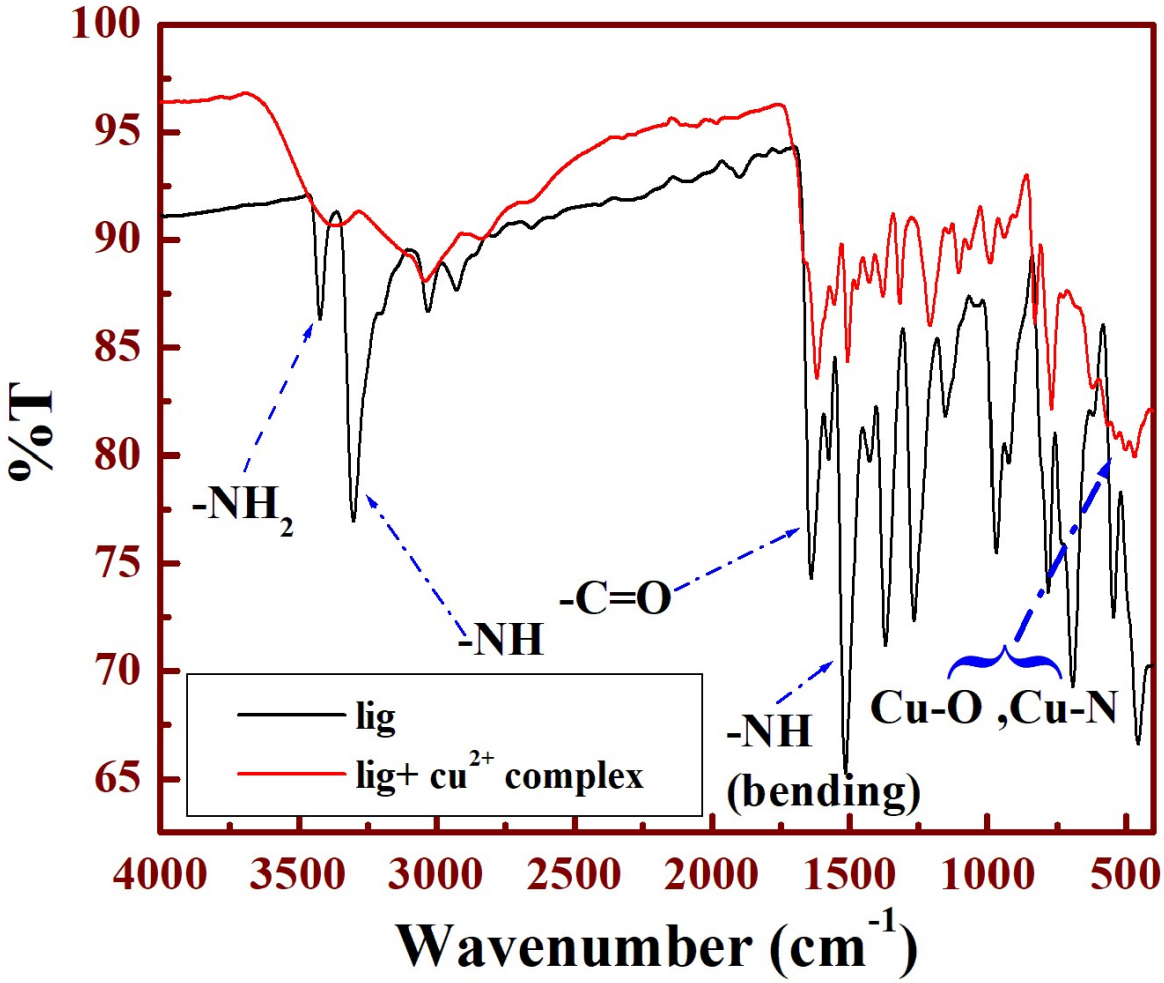

Fig. S4. IR spectrum of for **L²** and [**Cu(L²)Cl**] in solid state.

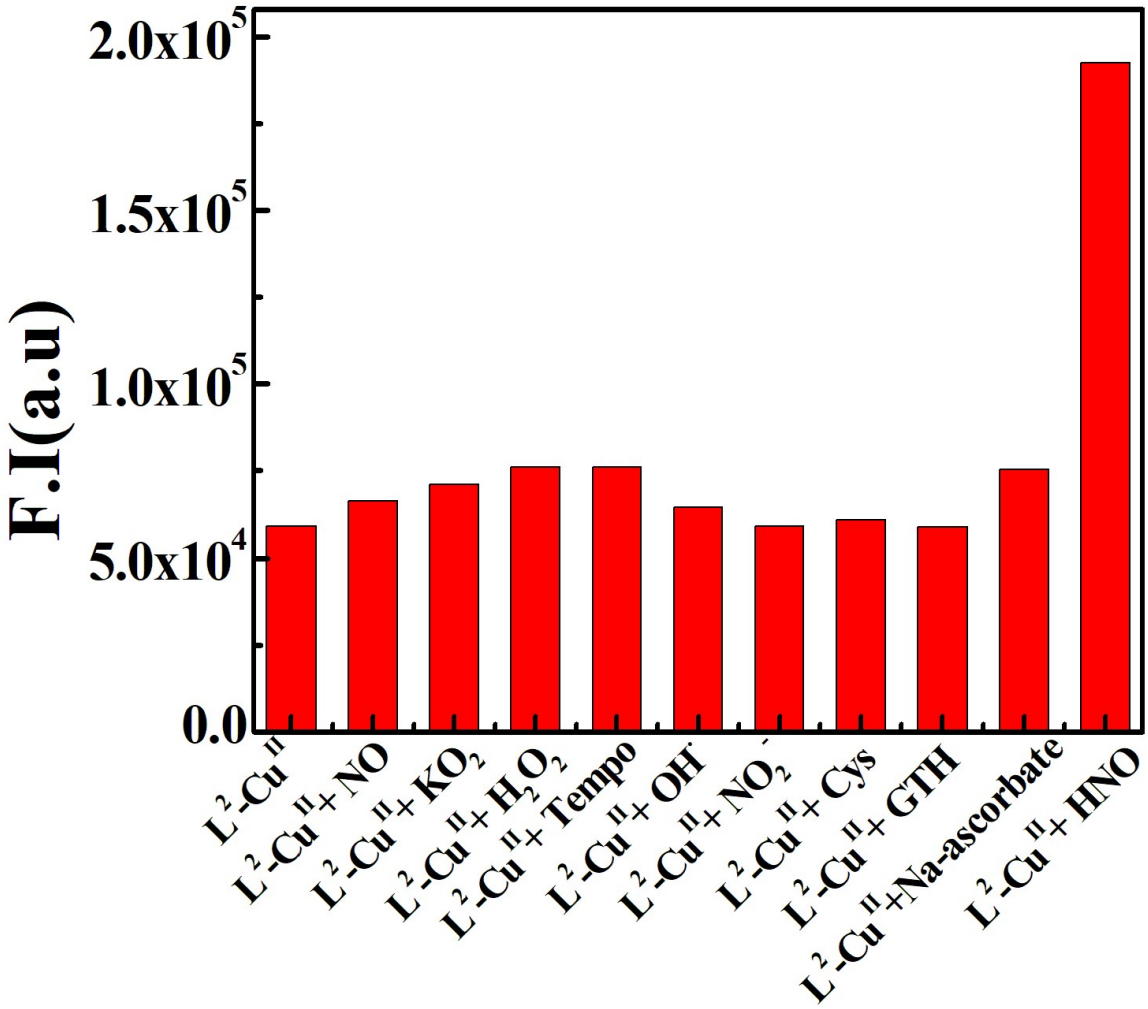

Fig.S5. Bar chart illustrating fluorescence responses of [**Cu^{II}-L^{2}**]$^{+}$ complexat 469 nm (λ_{ex} = 380 nm) towards different biological anions inCH_3CN. X^{n-} = NO , KO_2, H_2O_2 , TEMPO radical, OH· , NO_2^-, cysteine, glutathione, sodium ascorbate and HNO.

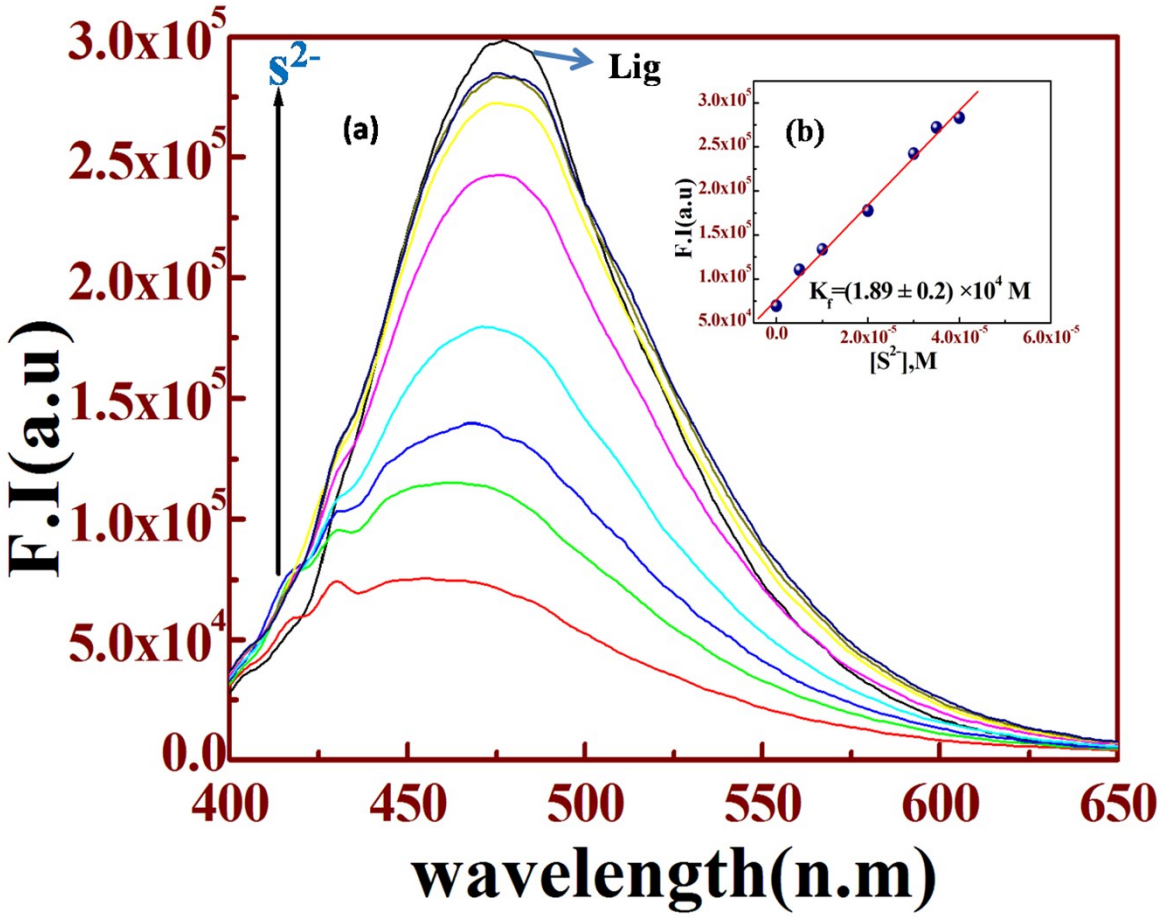

Fig.S6.(**a)** Fluorescence emission changes of **[**Cu^{II}-L^2**]**$^+$ (20 µM) in MeCN solutions upon addition of S^{2-}(50µM), λ_{ex}= 380nm, λ_{em}=478 nm);(b) Linear fitting plot.

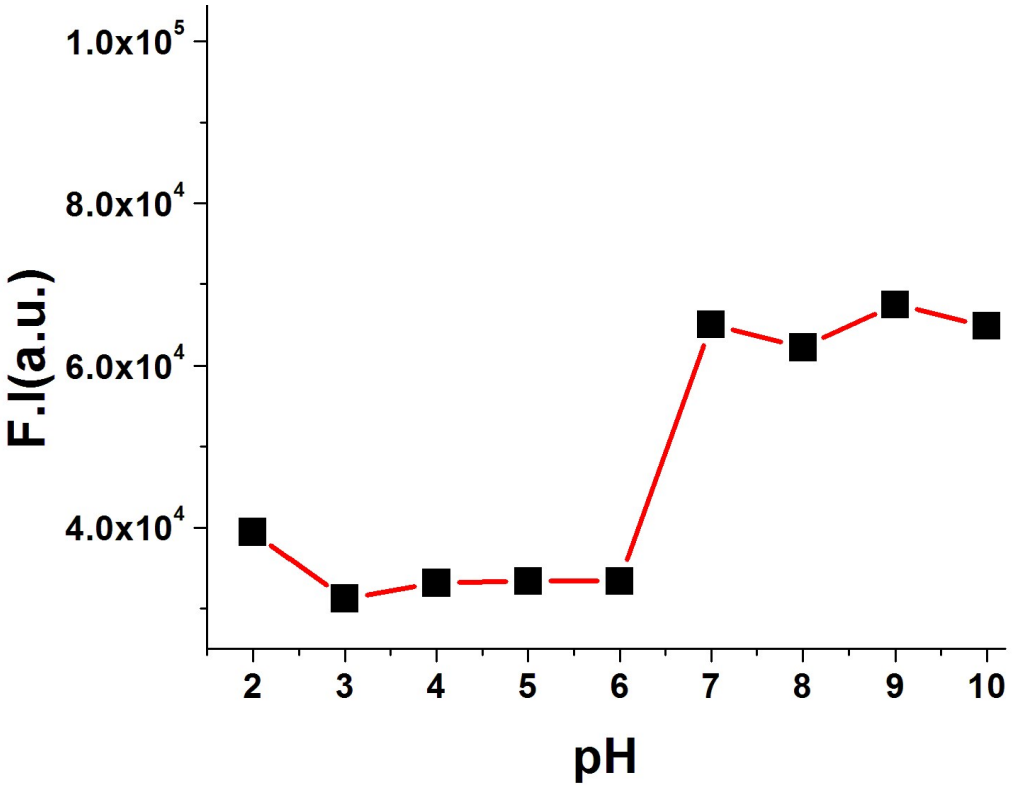

Fig. S7. pH dependence of fluorescence responses of [**Cu^{II}-L^{2}**]$^{+}$ complex.

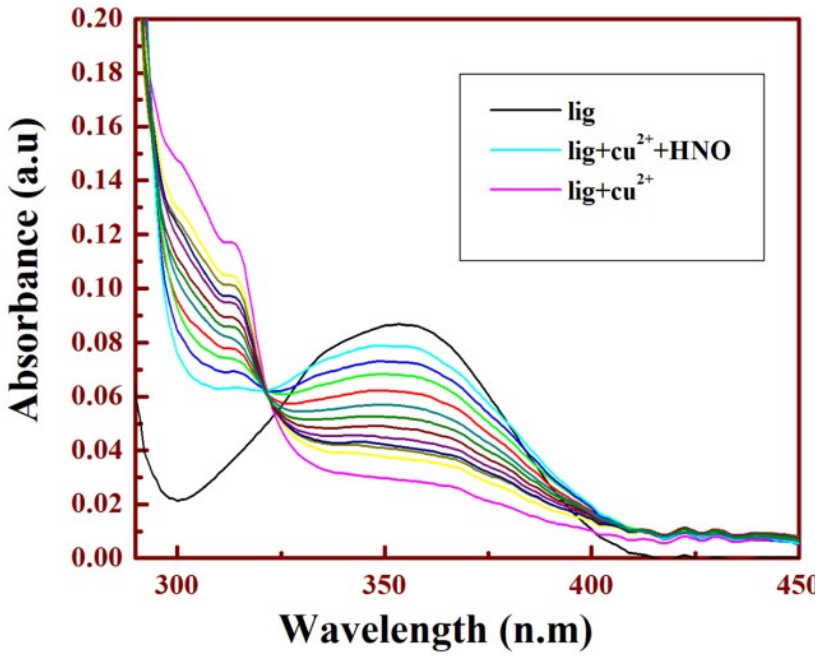

Fig. S8. Changes in UV-vis absorption spectra of **[**Cu^{II}-L^2**]**$^+$ (20 μM) in MeCN solutions with various amounts of HNO (0-2.5 equivalent).

Quantum Yield Determination:

Fluorescence quantum yields (**Φ**) were estimated by integrating the area under the fluorescence curves with the equation: $\Phi_{sample} = \frac{OD_{std}}{OD_{sample}} \times \frac{A_{sample}}{A_{std}} \times \Phi_{std}$

where, A was the area under the fluorescence spectral curve, OD was optical density of the compound at the excitation wavelength and η was the refractive indices of the solvent. Quantum yields of **L²** and [**Cu-L²**+ S^{2-}] and [**Cu- L²**+ HNO] complexes in acetonitrile (CH_3CN) are found to be 0.107, 0.09, 0.07 respectively using Quinine Sulphate as standard.

Table S1: Selective bond distance and bond angles of **L^2**

Bond distance(Å)		Bond-angles(°)	
N24-N26	**1.39**	C7 N17 C19	**129.776**
C22-O23	**1.25**	C19 C22 O23	**122.608**
C7-N17	**1.37**	C19 C22 N24	**117.167**
N17-C19	**1.45**	C22 N24 N26	**122.772**
C19-C22	**1.52**		
C22-N24	**1.37**		

Table S1a: Selective bond distance and bond angles of **[$Cu^{II}(L^2)Cl$].**

Bond distance(Å)		Bond-angles(°)	
Cu27-Cl29	**2.16**	N17Cu27O28	**84.356**
O28-Cu27	**1.90**	N17Cu27N16	**79.411**
N16-Cu27	**2.06**	O28Cu27Cl29	**101.149**
N17-Cu27	**2.24**	N16Cu27Cl29	**102.904**

Table S1b: Selective bond distance and bond angles of **[Cu^{I}(L^{2})].**

Bond distance(Å)		Bond-angles(°)	
N17-Cu27	**2.42**	N17Cu27O28	**85.02**
N16-Cu27	**1.91**	N17 Cu27 N16	**81.35**
O28-Cu27	**1.87**	N28C22N23	**125.17**
N23-N24	**1.40**		

Table S2: Selected parameters for the vertical excitation (UV-Vis absorptions) of **L^{2}**; electronic excitation energies (eV) and oscillator strength (f), configurations of the low-lying excited states of **L^{2}**; calculation of the $S_0 \rightarrow S_n$ energy gaps on optimized ground- state geometries (UV-vis absorption).

Electronic transition	Composition	Excitation energy	Oscillator Strength(f)	CI	Assignment	λ_{exp} (nm)
$S_0 \rightarrow S_6$	HOMO→LUMO+1	3.7365 eV	0.2682	0.25046	ILCT	350
$S_0 \rightarrow S_{14}$	HOMO-1 →LUMO+3	4.8318 eV	0.2029	0.37123	ILCT	256
$S_0 \rightarrow S_{31}$	HOMO-6 →LUMO+4	6.0349 eV	0.1193	0.35030	ILCT	200

Table S3 : Selected parameters for the vertical excitation (UV-Vis absorptions) of **[$Cu^{II}(L^2)Cl$]**; electronic excitation energies (eV) and oscillator strength (f), configurations of the low-lying excited states of **[$Cu^{II}(L^2)Cl$]**; calculation of the $S_0 \rightarrow S_n$ energy gaps on optimized ground- state geometries (UV-Vis absorption).

Electronic transition	Composition	Excitation energy	Oscillator Strength(f)	CI	Assignment	λ_{exp} (nm)
$S_0 \rightarrow S_{15}$	HOMO-1→LUMO	3.7383 eV	0.110	0.74643	ILCT/MLCT	352
$S_0 \rightarrow S_{17}$	HOMO-1→LUMO+1	3.8042 eV	0.0222	0.26103	ILCT/MLCT	315
$S_0 \rightarrow S_{38}$	HOMO-2→LUMO+1	4.9618 eV	0.0104	0.16877	ILCT/MLCT	256

Table S4 : Selected parameters for the vertical excitation (UV-VIS absorptions) of **[$Cu^{I}(L^2)$]**; electronic excitation energies (eV) and oscillator strength (f), configurations of the low-lying excited states of **[$Cu^{I}(L^2)$]**; calculation of the $S_0 \rightarrow S_n$ energy gaps on optimized ground- state geometries (UV-Vis absorption).

Electronic transition	Composition	Excitation energy	Oscillator Strength(f)	CI	Assignment	λ_{exp} (nm)
$S_0 \rightarrow S_4$	HOMO-2→LUMO	3.5366eV	0.0304	0.28325	ILCT/MLCT	350
$S_0 \rightarrow S_{12}$	HOMO-1→LUMO+2	4.2501eV	0.0183	0.56234	ILCT/MLCT	287